Experimental Study of Wave Propagation Dynamics of Binary Distillation Columns

Yng-Long Hwang, Glenn K. Graham, George E. Keller II
Union Carbide Corp., South Charleston, WV 25303

Jack Ting and Friedrich G. Helfferich
Dept. of Chemical Engineering, The Pennsylvania State University, University Park, PA 16802

High-purity distillation columns are typically difficult to control because of their severely nonlinear behavior reflected by their sharp composition and temperature profiles. The dynamic behavior of such a column, as characterized by the movement of its sharp profile, was elucidated by a nonlinear wave theory established previously. With binary alcohol mixtures, this study provides an experimental observation of such wave-propagation dynamics of a 40-tray stripping column and a 50-tray fractionation column in response to step disturbances of feed composition, feed flow rate, and reboiler heat supply. Our experimental results have verified that the sharp profile in a high-purity column moves as a constant-pattern wave and that the nonlinear wave theory predicts its velocity satisfactorily with very simple mathematics. Our results also demonstrate the asymmetric dynamics of the transitions between two steady states.

Introduction

Distillation columns producing high-purity products have attracted more and more attention owing to the growing demands of high product quality and minimal waste generation. By nature, a high-purity column is pinched near either or both column ends and exhibits severely nonlinear behavior as reflected by its sharp composition and temperature profiles. A major difficulty in control of such a column stems from its nonlinear dynamic phenomena, including high steady-state gains, large response lags, and strong dependence of gains and lags on disturbances (Luyben, 1971; Fuentes and Luyben, 1983; Kapoor et al., 1986; Skogestad and Morari, 1987). Another intriguing phenomenon is that the transition departing from the steady state with maximum separation is always faster, and usually much faster, than the return to it, as revealed by a few numerical simulations (Rose et al., 1956; Moczek et al., 1965; De Lorenzo et al., 1972; Mizuno et al., 1972; Weigand et al., 1972; Stathaki et al., 1985). This "asymmetric dynamics" implies that the most desirable steady state is intrinsically difficult to maintain.

For improving control of high-purity distillation columns, a few approaches exploiting the characters of their sharp profiles have attracted considerable interest. Observing the existence of a sharp temperature profile, Luyben (1972) pioneered a profile-position control strategy. It was reinvented and applied to plant columns by Boyd (1975) and later by Silberberger (1977), whose work was fortified by Gilles and Retzbach (1980) with a moving-front model. Viewing the movement of a sharp composition profile as a "wave" of a constant shape, Marquardt (1985, 1988) made a further advancement by using wave position and shape parameters as state variables in model-based control. Working on countercurrent separation processes in general, Hwang and Helfferich (1988) developed a nonlinear wave theory, which elucidates the development of "constant-pattern waves" (or "shock waves") governed by the phase equilibrium and their settlement to "standing waves" (steady-state profiles) owing to the column ends. The theory also analyzes the propagation of disturbances on nonuniform steady-state backgrounds, the interference of disturbance waves with background standing waves, and the asymmetric dynamics mentioned earlier (Hwang and Helfferich, 1989). It provides a theoretical basis for the control applications just cited that postulated *a priori* the existence of a constant-pattern wave. More recently, the theory was adapted to binary distillation (Hwang, 1991, 1995) by accounting for the side feeds and products as well as reflux and reboil. This adaptation clearly explains the nonlinear

Correspondence concerning this article should be addressed to Y.-L. Hwang.

phenomena of high steady-state gains, large response lags, their strong dependence on disturbances, and asymmetric dynamics. Conducting numerical simulations, Han and Park (1993) obtained very encouraging results from applying this theory to a profile-position control of a high-purity distillation column.

Although distillation dynamics has been extensively investigated for several decades, most previous studies relied on either mathematical models or simple input–output experiments, which recorded the response of a product composition or a temperature at a particular location to a given disturbance. Such experimental results are valuable in constructing lumped models for moderate-purity columns with relatively smooth profiles, but they are deficient in depicting the severely nonlinear behavior of high-purity columns. Among the few experimental efforts that attempted to observe dynamic behavior at multiple locations in a distillation column, Huckaba et al. (1963) tracked the individual composition histories of three trays and two products of a 12-tray binary distillation column in response to a step change of reflux ratio. For testing a computer simulation, Howard (1970) recorded the composition histories at 26 points in a 14-tray ternary distillation column during a startup under total reflux. Both studies focused on the responses at individual locations and paid little attention to the holistic behavior of the entire column.

With emphasis on the holistic behavior of high-purity columns, we reported earlier (Hwang et al., 1991) a preliminary experimental study of the wave-propagation dynamics of a laboratory distillation column with binary mixtures. This article presents a more extensive study on a glass column with 40–50 sieve trays. We tracked the movement of the temperature profile in the column during a transition from one steady state to another in response to a deliberately introduced step change of feed composition, feed flow rate, or reboiler heat supply. Our objectives were to confirm the existence of a constant-pattern wave in such a column and to verify the prediction of the wave velocity and the asymmetric dynamics by the nonlinear wave theory.

Theory

This section provides a brief review of the nonlinear wave theory for binary distillation columns established previously (Hwang and Helfferich, 1988, 1989; Hwang, 1991, 1995). With an analysis based on the vapor–liquid equilibrium properties, the theory demonstrates that the composition profile in each section of a typical binary distillation column exhibits a self-sharpening tendency. In a high-purity column, such a self-sharpening profile is relatively sharp and moves as a constant-pattern wave in response to a disturbance. The velocity of such a shock wave can be predicted using the information on the two sides of the wave (Hwang, 1995):

$$v_\Delta = v_{\Delta x} = v_{\Delta y} = \frac{(V''y'' - L''x'') - (V'y' - L'x')}{(W''x'' + U''y'') - (W'x' + U'y')}. \quad (1)$$

In this equation (see Notation for symbols), the wave velocity is defined on the basis of an upward distance coordinate; also, the superscripts $'$ and $''$ denote the lower and upper sides, respectively, of the wave. Since there is only one wave in each section of a binary distillation column, the velocity of such a wave can be predicted using the conditions at the two ends of that section.

For a high-purity distillation column, the steady state with maximum separation is of major interest in practice. At such a steady state, both column ends are pinched and the wave stands in the middle portion of the column. This steady state along with the standing wave has been referred to as "balanced" (Hwang and Helfferich, 1988) because the convective transports at equilibrium in the two countercurrent directions are balanced. For maintaining a balanced steady state, the primary concern is how the profile will move when the balanced condition is perturbed by disturbances. Considering a step disturbance at a column end, the nonlinear wave theory divides the dynamic response into two stages. In the first stage, the disturbance travels into the column on the background of the original standing wave until it merges into the latter. For a disturbance of composition, its velocity can be estimated with Eq. 1 (as an average velocity even if the disturbance wave is nonsharpening) by applying the original and new end conditions to the two sides of the disturbance wave. For a disturbance of flow rate, it typically propagates even faster than the bulk-flow velocity and therefore may be assumed to reach the standing wave in negligible time. In the second stage, the merger of the disturbance wave into the standing wave results in a new unbalanced wave, which travels toward a column end and thereby lowers the product purity at that end. Accordingly, we are mainly interested in predicting the initial velocity of the resulting main wave so that we can compensate the disturbance appropriately in order to maintain the sharp profile at its original location. Note that when the resulting wave is just formed, both sides of the wave (both column ends) are still pinched.

In a binary stripping or rectifying column, there exists only one wave, which is typically a simple constant-pattern wave. The velocity of such a wave can be calculated with Eq. 1 if the conditions of both leaving streams after the column is perturbed are given. Because of the pinched conditions at both column ends, the leaving stream compositions, x' and y'', can be calculated from x'' and y' with the equilibrium relation. These offer sufficient information to calculate molar holdups W' and U'' if the mass or volume holdups are given, but leave the leaving-stream flow rates L' and V'' unknown. These flow rates need to be either measured or estimated. The simplest estimation approach is to assume the molar flow rates of both liquid and vapor are uniform throughout the column (Hwang, 1991) if the heat loss from the column is small and the molar heats of vaporization of the two components are close. With this uniform-molar-flow (UMF) model, one needs to assume uniform molar holdups as well in order to maintain consistent material balances. For this model, Eq. 1 can be simplified by dropping the superscripts $'$ and $''$ from the flow rates and holdups:

$$v_\Delta = \frac{V\Delta y - L\Delta x}{W\Delta x + U\Delta y}. \quad (2)$$

If this simple approach turns out to be unsatisfactory, an improvement is to take the dynamic energy and overall material balances into account by tracking the wave velocity in

terms of molar enthalpy and holdup in addition to composition (Hwang, 1995):

$$v_{\Delta h} = v_{\Delta H} = \frac{(V''H'' - L''h'') - (V'H' - L'h') + Q_L}{(W''h'' + U''H'') - (W'h' + U'H')} \quad (3)$$

$$v_{\Delta W} = v_{\Delta U} = \frac{(V'' - L'') - (V' - L')}{(W'' + U'') - (W' + U')}. \quad (4)$$

Note that the energy balance, Eq. 3, includes the heat loss from the column Q_L. Now, L' and V'' can be solved from the following set of two linear equations:

$$v_{\Delta x} = v_{\Delta h} = v_{\Delta W}. \quad (5)$$

Application of this composition-and-enthalpy-wave (CEW) model to our experimental results will be illustrated later. In addition to these models, one may predict the initial velocity of a wave resulting from a disturbance of flow rate by using Eq. 1 with the column-end conditions all the same as at the original steady state except for the new flow rate of the entering stream and its exiting flow rate changed accordingly (because a flow-rate disturbance is assumed to propagate through the entire column at an instant).

For a two-section fractionation column, the entire profile consists of two waves. At a balanced steady state, both waves stand around the feed so that both column ends are pinched in a high-purity column. To such a steady state, the theory assumes that disturbances of the feed condition, the boilup rate, and the reflux rate reach and merge into the standing wave immediately. Once the balanced condition is perturbed, both waves tend to travel in the same direction—one moves toward and the other travels away from the feed. The former has fairly limited room to travel, whereas the latter travels across virtually the whole stripping or rectifying section. Thus, the latter is the principal wave that dictates the column dynamics and its initial velocity is of primary interest. As this wave travels toward a column end, the feed location soon becomes pinched and the wave establishes a constant shape and travels at a constant velocity, which is typically close to the initial velocity. The velocity of the constant-pattern wave can be calculated with Eq. 1 if the pinched section-end compositions and flow rates at the feed location are available. Given the measured temperatures around the feed location, these compositions and flow rates can be calculated with a vapor–liquid equilibrium model and material balances, as will be demonstrated later with our experimental results. For predicting the wave velocity using only the information of the original steady state and the disturbance, an operating-line approach was proposed previously (Hwang, 1991) for columns with a uniform molar flow rate in each section. If this assumption is invalid, the prediction of the conditions at the feed location may become relatively complicated. Instead, a simple approximation given below may be of more practical interest.

For many columns in practice, the operating reflux ratios are not much higher than the minimum values (usually 1.2–2.0 times of the latter). At a balanced steady state of such a column, the condition at the feed location is close to being pinched. Therefore, for the departure from such a steady state, one may disregard the contribution of the wave heading toward the feed and approximate the travel of the principal wave with the movement of the entire column profile. By viewing the latter as a composite wave, one can obtain its average velocity from a dynamic material balance around the entire column (Hwang, 1995):

$$v_{\Delta} = \frac{(V''y'' - L''x'') - (V'y' - L'x') - Fz_F}{(W''x'' + U''y'') - (W'x' + U'y')}. \quad (6)$$

For the initial wave velocity in response to a feed disturbance, Fz_F represents the new feed condition, which reaches the standing wave immediately, while all others remain the same as at the original steady state. If a disturbance of the boilup rate (or the reflux rate) is introduced, both V' and V'' (or L'' and L') should reflect the change because a flow-rate disturbance is assumed to affect the flow rate throughout the column immediately. The column-end compositions and flow rates at the original steady state can be derived from the measurable compositions and flow rates of the two product streams. A special consideration may be needed for the liquid holdups, which can be significantly different in the two sections. In Eq. 6, the denominator represents the change of component holdup due to the movement of the composition profile. Since the profile moves mainly in one section, it may be better to use the liquid mass (weight) or volume holdups in that section for calculating the molar holdups W' and W'' on both sides of the composite wave in spite that one side is in the other section. This approximation will also be demonstrated later with our experimental results.

Note that the nonlinear wave model is so simple in mathematics; other than the physical property relations, it needs at most three algebraic equations of material and energy balances for a section or an entire column. In contrast, a conventional dynamic model entails three differential balance equations for each tray or conceptual stage. Therefore, the nonlinear wave model is anticipated to predict the wave velocity only to a moderate accuracy (say, $\pm 50\%$ or even $\pm 100\%$). Its potential applications may include conceptual design, for which physical insight instead of accuracy is the primary concern, and model-based control, for which reliability and speed are usually more important than accuracy.

Experimental

We conducted our experiments of distillation dynamics on a laboratory glass column in two configurations. For simplicity, we started with a 40-tray stripping column to observe the fundamental behavior of a nonlinear wave. Specifically, our objectives were:

1. To verify the existence of a constant-pattern wave in a high-purity distillation column;
2. To test the prediction of the velocity of such a wave by the nonlinear wave theory in order to formulate a simple mathematical model of the nonlinear column dynamics;
3. To observe the asymmetric dynamics between the departure from and the return to a balanced steady state, and to compare the observation with the prediction by the nonlinear wave theory.

After these efforts, we reconfigured the apparatus to a 50-tray fractionation column with a feed introduced to tray 30 from

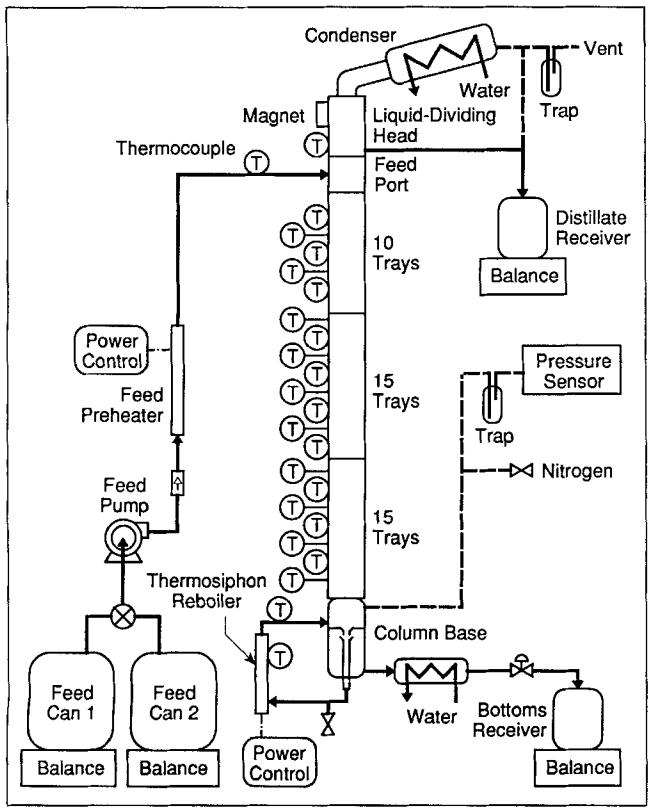

Figure 1. Laboratory stripping column for fundamental behavior of nonlinear wave propagation in distillation columns.

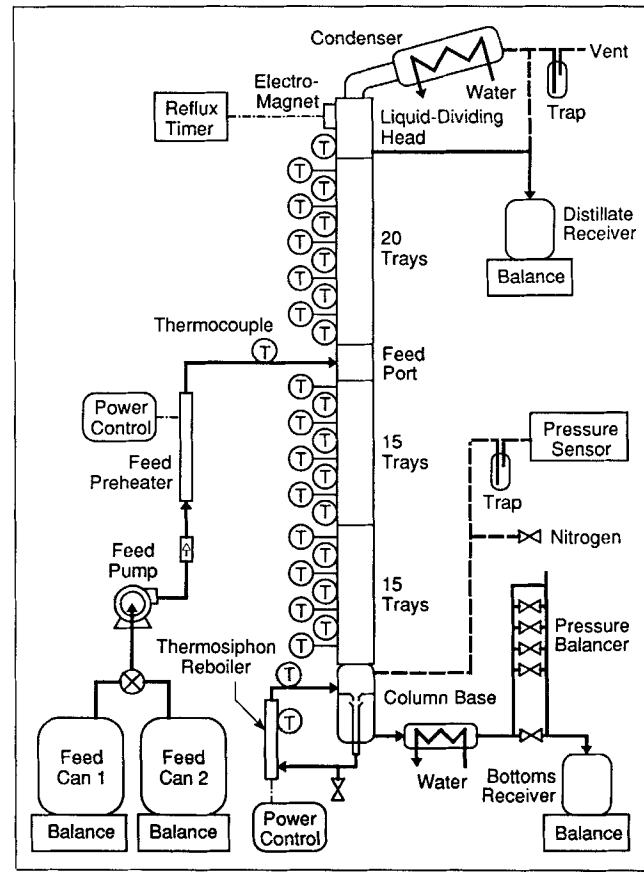

Figure 2. Laboratory fractionation column for wave-propagation dynamics of distillation columns.

the bottom to examine the wave-propagation dynamics in a situation of more practical interest.

Apparatus

Figures 1 and 2 show diagrams of our laboratory distillation apparatus in the two configurations, respectively. The column itself consisted of several vacuum-jacketed glass column segments with Oldershaw sieve trays of 50 mm in diameter and 25 mm in tray spacing (adaptation of LG-5631 from Lab Glass, Inc.). For monitoring the temperature profile of the column, we modified these Oldershaw segments by installing thermocouple wells on every other tray to measure the vapor temperatures. At the top, a glass total condenser was employed, and a glass liquid-dividing head (LG-6171 from Lab Glass, Inc.) was inserted below it for splitting the condensate into distillate product and reflux. For the stripping column, a permanent magnet was used for withdrawing all condensate as the distillate product (with no reflux); for the fractionation column, an electromagnet along with a timer was employed to control the reflux ratio. At the bottom, we designed a low-holdup thermosiphon reboiler consisting of a vacuum-jacketed glass column base and a set of four stainless-steel boiling tubes in parallel, which were heated with an electric heating tape and well insulated. The column base was designed to allow a major portion of the bottom product to be siphoned to the boiling tubes through a center pipe, and a minor portion overflowing the center pipe to be accumulated in the annular sump and drained out by the pressure difference resulting from the pressure drop through the loaded trays. To control the liquid level in the column-base sump, we initially used a needle valve to regulate the bottoms rate for the stripping column and later improved the mechanism with a multilevel pressure balancer for the fractionation column. Two feed cans were used for making a step change of the feed composition. The feed was transported by a high-precision metering pump (Digifeeder DF-165-C from IVEK Corp.) to the column through an in-line preheater, which was heated with an electric heating tape.

For data acquisition and device control, we built a program in an instrument-control software package (LabVEW 2.2 from National Instruments Corp.). We ran the program on a microcomputer (Macintosh Quadra 950 from Apple Computer, Inc.) to record the temperatures at various locations and the weights of feeds and products, and to control the heat supplies to the reboiler and the feed preheater. Each cycle of these actions took about 3 to 5 s. The temperatures were measured with type-T thermocouples, of which the voltage signals were amplified by a multichannel signal conditioner (SCXI 1300 from National Instruments Corp.) and then passed to the computer via an analog-to-digital converter. In addition to the tray temperatures, thermocouples were also installed to measure the temperatures of the feed, the heating-tape of the reboiler, the vapor in the reboiler, and the vapor in the liquid-dividing head. The weights of feeds and products were recorded by balances, whose digital signals

were read by the computer via a multiport digital interface. In the meantime, the computer sent control signals to two AC-voltage power controllers (Model 18DZ from Payne Engineering) to regulate the heat supplies to the thermosiphon reboiler and the feed preheater. We implemented a couple of PI (proportional-integral) feedback controllers in the program to control the reboiler at a chosen heating-tape temperature and the preheater at a selected feed temperature. For measuring the operating pressure and the pressure drop across the column, a pressure sensor (PX425-015AV from Omega Engineering, Inc.) was installed at the column base. In addition, a gas chromatograph (Model 5890 II from Hewlett-Packard Co.) with a capillary column (type DB-1 from J&W Scientific) was used for mixture composition analysis.

Materials

As an initial experimental study of the wave-propagation dynamics of distillation columns, our work has so far stayed within the scope of nearly ideal binary mixtures (following Raoult's law approximately) to avoid the complexities from thermodynamic nonideality. In the selection of such mixtures, we have also taken into consideration potential extensions to multicomponent mixtures, including both ideal mixtures and nonideal ones possibly with azeotropes. With these criteria and concerns of safety and other practical aspects, we chose the compounds in the lower portion of the alcohol homologous series for the following reasons:

- Physical properties of these alcohols and their binary mixtures are well studied and documented (Daubert and Danner, 1991; Gmehling et al., 1977).
- Their binary mixtures are nearly ideal with respect to vapor–liquid equilibrium, and thus fit in our current work. Moreover, they can constitute nearly ideal multicomponent mixtures and nonideal (including azeotropic) ones with water, therefore may be good choices for future multicomponent experiments.
- Among organic chemicals, they are relatively safe to human health and the environment.
- They have normal boiling points in a proper range for handling with laboratory equipment, for boiling and condensing at ambient pressure, and for measuring with regular thermocouples.

In the present study, we worked with methanol/1-propanol and methanol/1-pentanol binary mixtures for proper relative volatilities. The physical properties of these compounds and mixtures are given in Table A1 (Appendix A). We used alcohol materials with purity above 99% (from Aldrich Chemical Co.).

Measurements and procedures

Pressure. For simplicity, we conducted all our experiments at ambient pressure, which usually falls between 740 and 760 mm Hg at our location. We monitored the base pressure at all times. Since the head pressure was the same as the base pressure when the column was empty, we calculated the pressure drop across the column by taking the difference between the base pressure when a hydraulic steady state was established and that before the startup or the difference between the base pressure at the last steady state and that after the shutdown.

Reboiler Characteristics. We determined the effective reboiler heat supply Q_B (net boilup energy) with pure 1-propanol in an assembly with the same ancillary equipment as shown in Figure 1 but without the tray segments. The feed port was placed immediately on the column base and underneath the liquid-dividing head. Since the electric power source usually varied a few percent during a day, we set a fixed heat supply by maintaining the heating-tape temperature T_Q at a specified set point with feedback control. To maintain a constant holdup in the reboiler, we fed 1-propanol at 95°C (about 2°C below its boiling point) at a proper rate to keep a liquid level of 5–7 cm in the column-base sump, from which no liquid was withdrawn. After the process had attained a steady state at a specific T_Q, we measured the distillate rate (no reflux). Neglecting the heat loss from the part above the column base, we viewed the distillate rate as equal to the boilup rate and calculated Q_B based on this rate and the heat of vaporization of 1-propanol at the operating pressure, 759 mm Hg (at which the boiling point was 97.1°C). We established a calibration curve of Q_B vs. the heat-transfer driving force, that is, the difference between T_Q and the boiling temperature (reboiler vapor temperature T_0). Within our operating range, this curve turned out to be an excellent straight line, which implied a constant lumped heat-transfer coefficient of the reboiler. In addition to the boilup rate, we also measured the reboiler holdup (excluding the column-base sump) by weighing the liquid drained out of the boiling tubes after shutting down the operation from the steady state with a specific heat supply. It turned out that there was no significant dependence of the holdup on the heat supply, and the average holdup of the reboiler within our operating range was 50 g.

Input Variables. In our dynamic experiments, we attempted to observe the response of the entire column to a step change of feed composition x_F, feed flow rate F, or reboiler heat supply Q_B. We chose a reference feed composition of equal moles ($x_F = 0.5$) to obtain easily measurable temperature profiles and product flow rates. For conservation of material, we prepared a feed by recombining the products collected from a previous run and adjusting its composition with the aid of a gas chromatograph. This gave a feed composition within ± 0.002 of the specified mole fraction. For the feed flow rate, we prescribed a reference value based on a stripping-section tray loading of 10–20% of the flooding vapor velocity predicted with the correlation of Fair (1961). We relied on the high-precision metering pump to maintain a constant mass (weight) flow rate F_w of the feed with less than $\pm 1\%$ fluctuation. Although a saturated liquid feed was preferable, it is difficult in practice to preheat the feed to its bubble point without the risk of partial vaporization. To avoid this, we used a PI feedback controller to maintain the temperature T_F of the feed at 3–7°C below its bubble point measured or predicted with the physical property models (see Appendix A).

In this study, we operated the stripping column without reflux and the fractionation column with a fixed reflux ratio. With the reference feed condition and reflux ratio, a reference reboiler heat supply was selected in accordance with a balanced steady state, which will be referred to as a steady

state B for convenience. A steady state with a standing wave closer to the bottom will be denoted by A, and one with a wave closer to the top will be denoted by C. The effective reboiler heat supply was kept constant by using a PI feedback controller to regulate the heating-tape temperature within 1°C around its set point. We maintained a constant liquid level in the column-base sump in the range of 4–10 cm by adjusting the drainage valve for the stripping column and by selecting a proper channel of the pressure balancer for the fractionation column. This kept the reboiler characteristics consistent with the calibration line for the effective heat supply, and also automatically regulated the bottoms flow rate.

Input Disturbances. Since we were interested in both wave propagation and asymmetric dynamics, each of our dynamic experiments consisted of a pair of transitions between a steady state B and either a steady state A or C. We initiated a transition by introducing a 5–10% near-step change of one of the three selected input variables while maintaining all others constant. We generated a step change of the feed composition by switching from one feed can to the other with a composition difference of 5 mol%, and that of the feed flow rate by altering the pump speed. The ideality of these sharp step changes was slightly softened by the fact that the feedback control of the feed preheater took 2–5 min to compensate the accompanied change of the feed temperature. In addition, the feed composition change was inevitably delayed by 1–2 min owing to the transportation from the feed can to the feed port of the column. We created a near-step change of the reboiler heat supply by changing the set point of the heating-tape temperature, which typically overshot the new set point in 2 min and settled at that temperature in about 5 min.

Monitoring and Data Acquisition. To monitor the dynamic behavior of the entire column, we implemented in our data-acquisition program a capability of tracking the movement of the temperature profile during a transition from one steady state to another. As the thermocouples being scanned in cycles of 3–5 s, our program plotted on the computer monitor three snapshots of the temperature profile: the current one along with two recorded several minutes earlier. The program also stored these data to a file at chosen time intervals. In addition, it showed several histograms for interactively selected variables. One histogram was used to monitor the most sensitive tray temperature (the one at the sharpest part of the temperature profile) when a steady state was approached. At the beginning and the end of a transition, we ensured the attainment of a steady state by keeping such a temperature on a flat trend for at least 20 min.

The program also recorded the weights of feed, distillate, and bottoms in each cycle, and calculated the flow rates based on weight changes in corresponding time intervals. The feed rate was used to check the performance of the feed pump, and the distillate rate is essential in analyzing the dynamic behavior of the column. The product compositions are also needed for calculating the wave velocity. We collected distillate and bottoms samples at both initial and final steady states and analyzed their compositions with a gas chromatograph.

Column Holdup. In addition to the compositions and flow rates, tray holdups are also required for calculating the wave velocity. For our column under ambient pressure, the vapor holdup is negligible compared with the liquid holdup. Since a direct measurement of the liquid holdups on the trays during a run is impractical, we took an indirect approach by measuring the entire column holdup at a steady state. After the final steady state in each run had been attained, we first drained the liquid in the column base sump, and then immediately turned off the feed and product streams as well as the heat supplies. Following a period of cooling down, all liquid on the trays and in the reboiler was collected in the column-base sump and the boiling tubes. By weighing this lumped liquid and subtracting the holdup of the reboiler (50 g), we obtained the total mass holdup of all trays at the final steady state. It turned out that there was no apparent difference among the holdups at steady states of different types (A, B, or C). This result was supported by virtually the same pressure drop at these steady states.

Stripping column experiments

Using the 40-tray stripping column as shown by Figure 1, we conducted three pairs of dynamic experiments (runs S1 to S6) with the methanol/1-propanol binary mixture. The operating conditions of these experiments are given in Table 1. The steady states of type B represent the reference conditions for these experiments: $x_F = 0.50$, $F = 40$ mol/h, $T_F = 70$°C (the bubble point is 76°C), and $Q_B = 1{,}121$ kJ/h.

In each run, we first established an initial steady state, then introduced a step change and maintained the new condition until a final steady state was attained. In run S1, we established the reference steady state B, and then moved the temperature wave up by switching the feed to one with $x_F = 0.45$. To maintain a constant feed flow rate in terms of moles instead of weight, we also adjusted the feed-pump speed accordingly at the same moment. Also, to keep approximately the same temperature difference from the bubble point of the feed (77°C for $x_F = 0.45$), we raised the set point of the feed temperature to 71°C. In run S2, we began with an effort to reproduce the final steady state C of run S1, and then introduced the opposite step change to restore the steady-state B. We conducted the other pairs of runs in the same fashion. In runs S3 and S4, we changed the feed flow rate between 40 and 38 mol/h; we had to provide a little higher heat supply to the reboiler to obtain the reference steady state B, likely because of a little lower room temperature (and thus higher heat loss) at that time. In run S5, we moved the temperature wave down from the steady state B by reducing the heating-tape temperature T_Q from 189°C to 184°C. For most of the transition, the reboiler vapor temperature T_0 remained at 97.8°C until the final steady state A was approached. To show the step change of Q_B, Table 1 presents its values calculated with $T_0 = 97.8$°C, instead of the actual T_0, for steady states A of runs S5 and S6.

Fractionation column experiments

After the stripping column experiments, we reconfigured the apparatus to a 50-tray fractionation column as shown by Figure 2. We carried out a couple of dynamic experiments (runs F1 and F2) with the methanol/1-propanol binary mixture, but we found that this system had a difficulty to maintain pinches at both column ends. Thus, we changed the mixture to the methanol/1-pentanol system and conducted two more pairs of dynamic experiments (runs F3–F6). In all of

Table 1. Operating Data of Dynamic Experiments on Stripping Column with Methanol/1-Propanol Binary Mixture

Run Number	S1	S2	S3	S4	S5	S6
Input variables	x_F	x_F	F	F	Q_B	Q_B
Changed variables	x_F, F_w, T_F	x_F, F_w, T_F	F_w, F	F_w, F	T_Q, Q_B	T_Q, Q_B
Head pressure (mm Hg)*	745	750	744	743	746	746
Pressure drop (mm Hg)	29	29	29	29	29	29
Liquid column holdup (g)**	240	242	241	245	247	243
Initial Steady State						
Type	B	C	B	C	B	A
x_F	0.500	0.450	0.500	0.500	0.500	0.500
F_w (g/h)	1,844	1,898	1,844	1,753	1,842	1,841
F (mol/h)†	40.0	40.0	40.0	38.0	40.0	40.0
T_F (°C)	70.2	71.3	70.6	70.2	70.1	70.3
T_0 (°C)	97.7	97.9	97.7	97.7	97.8	96.9
T_Q (°C)	189.0	189.0	189.9	190.1	189.0	184.3
Q_B (kJ/h)††	1,122	1,119	1,137	1,139	1,121	1,048
x_B	0.000	0.000	0.000	0.000	0.000	0.019
D_w (g/h)	946	936	953	922	948	917
D (mol/h)†	25.1	24.0	25.2	24.4	25.1	24.3
T_{40} (°C)	76.1	78.1	76.0	76.3	76.1	76.0
x_D	0.799	0.754	0.796	0.794	0.799	0.799
Final Steady State						
Type	C	B	C	B	A	B
Time elapsed (min)	210	340	180	300	180	300
x_F	0.450	0.500	0.500	0.500	0.500	0.500
F_w (g/h)	1,900	1,839	1,746	1,839	1,840	1,845
F (mol/h)†	40.0	39.9	37.9	39.9	39.9	40.1
T_F (°C)	71.2	70.2	70.2	70.4	70.2	70.3
T_0 (°C)	97.8	98.0	97.7	97.7	96.8	97.8
T_Q (°C)	189.0	189.0	190.9	190.0	184.3	189.1
Q_B (kJ/h)††	1,121	1,119	1,138	1,138	1,048	1,122
x_B	0.000	0.000	0.000	0.000	0.019	0.000
D_w (g/h)	940	941	923	946	920	945
D (mol/h)†	24.1	24.9	24.3	25.1	24.5	25.1
T_{40} (°C)	78.2	76.5	76.5	75.9	76.1	76.1
x_D	0.751	0.795	0.786	0.800	0.803	0.799
Transition Period for Calculating Wave Velocity						
Time elapsed (min)	20–60		10–40		10–40	
x_F	0.450		0.500		0.500	
F_w (g/h)	1,902		1,748		1,840	
F (mol/h)†	40.1		37.9		39.9	
T_0 (°C)	97.7		97.7		97.7	
Q_B (kJ/h)††	1,123		1,139		1,048	
x_B‡	0.000		0.000		0.000	
D_w (g/h)	944		938		903	
D (mol/h)†	24.4		24.8		24.0	
T_{40} (°C)	77.6		76.2		76.2	
x_D‡‡	0.762		0.796		0.799	

*Assumed to remain the same value as before startup, which was the same as the base pressure at that time (the variation in a run was within 3 mm Hg).
**Measured for the final steady state.
†Calculated from the measured mass-flow rate and the mixture molecular weight.
††Calculated from $T_Q - T_0$; calculated with $T_0 = 97.8$°C (the same as at steady-state B) for steady states A of runs S5 and S6 to represent Q_B during most of the transition except near steady-state A (the actual values at steady states A were 1,064 and 1,062 kJ/h for runs S5 and S6, respectively).
‡Assumed to remain the same as at the initial steady state.
‡‡For run S1, assumed to be the same as that measured in a test run with $x_F = 0.45$ and the top end pinched; for runs S3 and S5, assumed to remain the same as at the initial steady state because the top end was still pinched.

these experiments with fixed reflux ratios, we focused on the wave propagation dynamics in the stripping section. Table 2 lists the operating conditions at the initial and final steady states of these experiments. For runs F3–F6, the reference conditions at the balanced steady state B were $x_F = 0.50$, $F = 30$ mol/h, $T_F = 74$°C (the bubble point is 79°C), $R = 0.25$, and $Q_B = 1{,}068$–$1{,}103$ kJ/h with a little adjustment to compensate for the variation of the heat loss due to different room temperatures. The reflux ratio was set by a timer with a time ratio of 4 to 16 s. With this low reflux ratio, we observed that the trays in the rectifying section were very lightly loaded. Although this might imply a low tray efficiency in that section, it still produced very pure distillate product, and it had little impact on the behavior of the stripping section.

In run F3, we moved the temperature wave down from the steady state B by changing the feed composition to $x_F = 0.55$ while maintaining a constant feed flow rate in terms of weight instead of moles, as for typical columns in practice. This, however, introduced an accompanied step change of the molar feed flow rate. In addition, we reduced the feed tempera-

Table 2. Operating Data of Dynamic Experiments on Fractionation Column with Methanol/1-Propanol and Methanol/1-Pentanol Binary Mixtures

Run Number	F1	F2	F3	F4	F5	F6
Mixture*	C_1/C_3	C_1/C_3	C_1/C_5	C_1/C_5	C_1/C_5	C_1/C_5
Input variables	x_F	x_F	x_F, F	x_F, F	Q_B	Q_B
Changed variables	x_F, F_w	x_F, F_w	x_F, T_F	x_F, T_F	T_Q, Q_B	T_Q, Q_B
Head pressure (mm Hg)**	740	743	753	750	748	746
Pressure drop (mm Hg)	36	36	24	24	24	24
Liquid column holdup (g)†	236	248	188	198	194	195
Reflux ratio, R	1.5	1.5	0.25	0.25	0.25	0.25
Initial Steady State						
Type	B	A	B	A	B	A
x_F	0.500	0.550	0.500	0.550	0.500	0.500
F_w (g/h)	1,101	1,070	1,805	1,815	1,794	1,814
F (mol/h)††	23.9	24.0	30.0	31.7	29.9	30.2
T_F (°C)	72.0	72.1	73.9	72.2	74.1	74.1
T_{30} (°C)‡	76.3	72.7	82.7	76.3	82.9	78.3
T_0 (°C)	98.3	96.4	139.3	139.0	139.0	139.0
T_Q (°C)	198.0	197.9	227.0	227.1	229.0	223.1
Q_B (kJ/h)‡‡	1,252	1,251	1,067	1,072	1,102	1,009
x_B	0.0003	0.0003	0.0004	0.0004	0.0004	0.0004
D_w (g/h)	379	403	482	553	476	480
D (mol/h)††	11.8	12.6	15.0	17.3	14.8	15.0
T_{50} (°C)	63.7	63.7	64.0	63.8	64.0	63.8
x_D	0.9997	0.9995	0.9992	0.9997	0.9989	0.9994
T_{32} (°C)			74.8		75.2	
Final Steady State						
Type	A	B	A	B	A	B
Time elapsed (min)	420	540	210	360	210	300
x_F	0.550	0.500	0.550	0.500	0.500	0.500
F_w (g/h)	1,069	1,105	1,818	1,810	1,811	1,816
F (mol/h)††	23.9	24.0	31.7	30.1	30.1	30.2
T_F (°C)	72.2	71.7	72.2	74.1	74.0	74.0
T_{30} (°C)‡	72.6	77.2	76.5	83.2	78.3	84.1
T_0 (°C)	96.6	98.2	139.5	139.1	138.6	139.0
T_Q (°C)	198.0	197.9	227.1	227.0	223.1	229.1
Q_B (kJ/h)‡‡	1,252	1,253	1,065	1,069	1,011	1,104
x_B	0.0003	0.0000	0.0005	0.0000	0.0005	0.0000
D_w (g/h)	410	386	560	490	483	485
D (mol/h)††	12.8	12.0	17.5	15.3	15.1	15.1
T_{50} (°C)	63.5	63.8	63.7	64.0	64.0	64.2
x_D	0.9999	0.9988	0.9996	0.9992	0.9995	0.9987
Transition Period for Calculating Wave Velocity						
Time elapsed (min)			10–40		10–40	
x_F			0.550		0.500	
F_w (g/h)			1,796		1,789	
F (mol/h)††			31.4		29.8	
T_F (°C)			72.1		74.0	
T_{30} (°C)‡			76.7		78.6	
T_0 (°C)			139.4		139.0	
Q_B (kJ/h)‡‡			1,066		1,010	
x_B§			0.0004		0.0004	
D_w (g/h)			527		458	
D (mol/h)††			16.4		14.3	
T_{50} (°C)			64.0		64.0	
x_D§			0.9992		0.9989	
T_{32} (°C)			70.0		71.3	

*C_1 = methanol, C_3 = 1-propanol, and C_5 = 1-pentanol.
**Assumed to remain the same value as before startup, which was the same as the base pressure at that time (the variation in a run was within 3 mm Hg).
†Measured for the final steady state.
††Calculated from the measured mass-flow rate and the mixture molecular weight.
‡Feed tray temperature.
‡‡Calculated from $T_Q - T_0$; calculated with T_0 = 98.3 and 98.2°C (the same as at steady-state B) for steady states A of runs F1 and F2 to represent Q_B during most of the transition except near steady-state A (the actual values at steady states A were 1,279 and 1,281 kJ/h for runs F1 and F2, respectively).
§Assumed to remain the same as at the initial steady state.

ture to 72°C in order to keep the same temperature difference from the bubble point (77°C for $x_F = 0.55$). In run F4, we reversed the change of the feed conditions to observe the returning transition from the steady state A to B. In runs F5 and F6, we introduced step changes of the reboiler heat supply by changing the reboiler heating temperature T_Q to observe similar constant-pattern wave behavior and asymmetric dynamics.

Results and Discussion

Stripping column dynamics

Figures 3–5, each including a pair of graphs, present the recorded snapshots of temperature profiles at various times in our dynamic experiments S1–S6 on the 40-tray stripping column with the methanol/1-propanol binary mixture. Each graph demonstrates the movement of the temperature profile in the transition from one steady state to another initiated by a step change of feed composition, feed flow rate, or reboiler heat supply. In each pair of these figures, the left graph (a) shows the transition departing from a balanced steady state while the right graph (b) illustrates the returning transition. Figure 6 gives the histories of the measured distillate flow rates in these runs. The measured operating conditions at the initial and final steady states are given in Table 1. For calculating wave velocities, Table 1 also includes the measured column-end conditions during a period within the first hour of runs S1, S3, and S5.

Constant-Pattern Wave. The transient temperature profiles in Figures 3–5 clearly demonstrate the propagation of a constant-pattern wave in our stripping column. For a wave initiated by a step change of the feed composition at the top, Figure 3a shows that the disturbance wave propagated downward and took about 10 min to reach and merge into the balanced standing wave, then the resulting wave traveled upward at a fairly constant velocity within the first hour. After the first hour, the top end was no longer pinched and the wave was gradually slowed down by the nonequilibrium column-end effect, as explained by the nonlinear wave theory (Hwang and Helfferich, 1988; Hwang, 1991). As illustrated by Figures 4a and 5a, similar nonlinear wave behavior was observed for waves resulting from step changes of the feed flow rate at the top and the boilup rate (reboiler heat supply) at the bottom, except that these disturbances reached the initial standing wave in negligible time. In both cases, the resulting wave traveled at a constant velocity within the first 40 min of each transition.

Wave Velocity. For maintaining the column subject to disturbances at a balanced steady state, the velocity of the re-

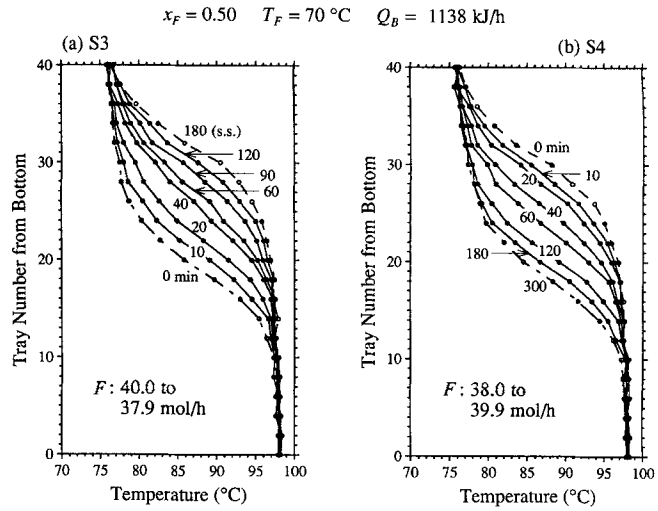

Figure 4. Temperature wave in stripping column with methanol / 1-propanol in response to step change of feed flow rate: (a) departure from balanced steady state; (b) return to balanced steady state.

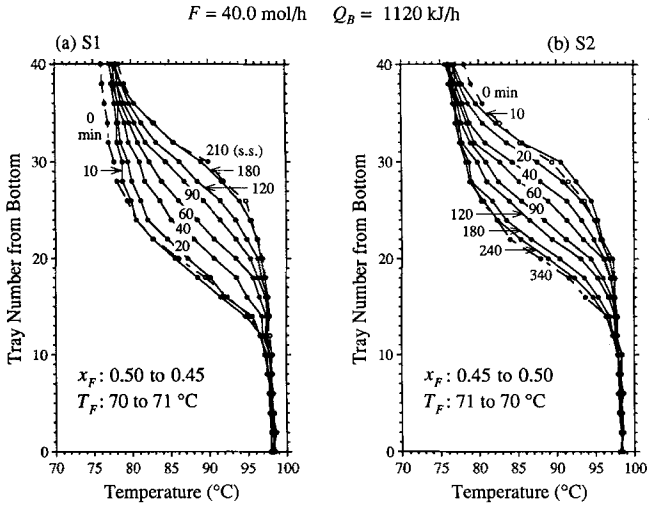

Figure 3. Temperature wave in stripping column with methanol / 1-propanol in response to step change of feed composition: (a) departure from balanced steady state; (b) return to balanced steady state.

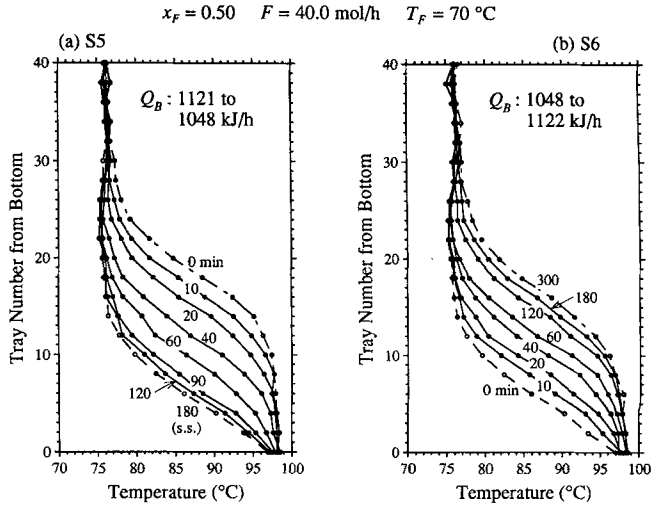

Figure 5. Temperature wave in stripping column with methanol / 1-propanol in response to step change of reboiler heat supply: (a) departure from balanced steady state; (b) return to balanced steady state.

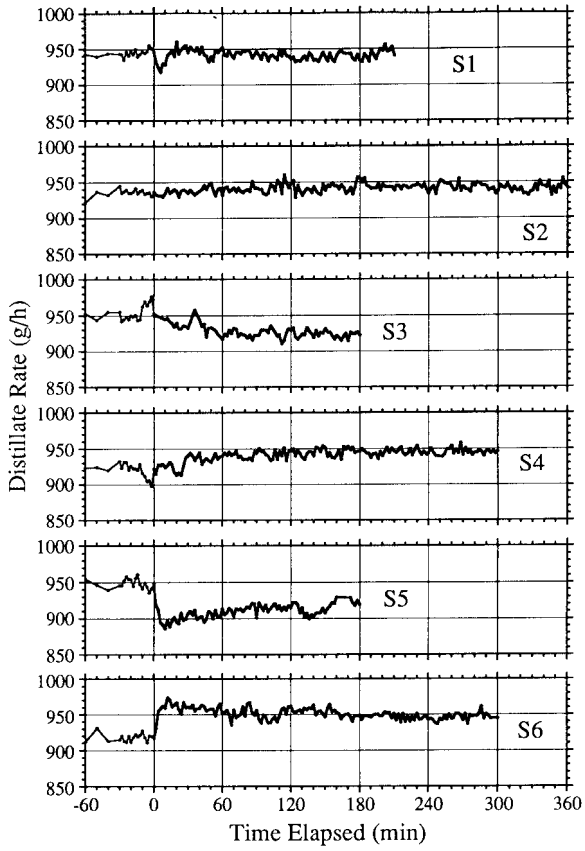

Figure 6. Histories of distillate rate in dynamic experiments on stripping column with methanol/1-propanol.

sulting wave when it is just formed is of primary interest, as mentioned in the Theory section. However, it is impractical to measure the wave velocity at a single instant. Instead, for runs S1, S3, and S5, we measured the average velocity over a period when the wave traveled at a fairly constant speed according to the recorded temperature profiles. For such a period, we chose 20–60 min of time elapsed for run S1 and 10–40 min for runs S3 and S5. The measured column-end conditions in these periods are given in Table 1 and the measured wave velocities based on the recorded temperature profiles are listed in Table 3.

Using the measured compositions and flow rates at the column ends, one can calculate the wave velocity with Eq. 1, as illustrated in Appendix B. The calculated results are given in Table 3. The calculated velocity for the initial standing wave represents the measurement errors for flow rates as well as compositions. For all three runs, the calculated velocity of the resulting wave is about 20% higher than the measured velocity (the percentage error in Table 3 is defined based on the absolute value of the wave velocity). This error is reasonable for a dynamic phenomenon with high sensitivity by nature and initiated by a mere 5–10% change of an input variable. The error can be attributed to either the experimental errors or the simplifying assumption of the liquid tray holdups or both. The major experimental errors were most likely on the column holdup and the boilup rate V', but the latter is inconsequential here because y' is essentially zero. Since the velocity error appears to be systematic, we suspect that it is mainly related to the tray holdups, resulting from either the measurement of the column holdup or the assumption of uniform mass holdups. For the disturbance wave in run S1, the calculated velocity states that it would take 12 min to reach the initial standing wave if one viewed the latter as a step at tray 19 (Hwang and Helfferich, 1988). This is fairly close to the result based on the recorded temperature profiles.

Prediction of Wave Velocity. The preceding calculation relies on the column-end conditions measured during the transition. What is of more practical interest is a model that predicts the wave velocity with only the information of the initial steady state and the step disturbance. Examples are the UMF and CEW models presented in the Theory section. Because the leaving-stream compositions x' and y'' either remain the same as at the initial balanced steady state or can be calculated with a vapor–liquid equilibrium relation, the major task of these models is to predict the leaving-stream flow rates L' and V''. For a stripping column, V'' is of major interest. The UMF model assumes that V'' remains the same as at the initial steady state unless V' is changed by a change of the reboiler heat supply (see Appendix B). Table 3 reveals that this incurs an error up to $\pm 3\%$ for these runs. Owing to the high sensitivity of the nonlinear wave, however, this leads to an overprediction of the wave velocity by 100–200%. Part of this error can be attributed to the assumption of uniform molar tray holdups, which is somewhat unrealistic but is required to maintain the consistency of material balances under the assumption of uniform molar flows. Figure 6 shows that the distillate flow rate V'' was indeed changed by the step change of either input variable (there was no apparent change of the mass flow rate for runs S1 and S2 with a feed composition change, but the molar rate did change because of a change in the distillate composition). This indicates a need for a better prediction of V'' of this column.

An improvement can be obtained by employing the CEW model (see Appendix B for details). This model takes the column heat loss Q_L into account in the dynamic energy balance, Eq. 3. For simplicity, we let Q_L include the energy consumed to heat the feed from a slightly subcooled temperature to its bubble point. The Q_L at the initial steady state can be calculated using the steady-state material and energy balances with the measured V''. It turns out that the heat loss amounts to about 13% of the reboiler heat supply (see Table 3). This Q_L should be a good approximation for that at the moment when the resulting wave was just formed. However, the wave velocity was measured over a period in which the temperature profile had shifted. To get a fair comparison between the predicted and measured wave velocities, we adjust Q_L according to the ratio of the average column temperature at the middle of the measuring period (e.g., 40-min time elapsed for run S1) to that at the initial steady state. Table 3 gives the predictions by the CEW model both with and without the heat-loss adjustment. With the heat-loss adjustment, the CEW model results in a V'' with an error of $\pm 1.5\%$ or smaller, but overpredicts the velocity of the main wave by 60–85%. If we compare it against the wave velocity calculated with the measured column-end conditions to exclude the possible systematic errors on the tray holdups, the CEW model overpredicts the main wave velocity by 30–50%. These overpredictions may primarily result from the fact that the

Table 3. Velocities of Constant-Pattern Waves in Stripping Column

Run No.	S1	S1	S3	S5
Initial Steady State				
W' (mol/tray)		0.101	0.101	0.101
W'' (mol/tray)		0.132	0.132	0.132
v_Δ calculated (tray/h)		0.7	1.1	1.5
Wave	Disturbance	Main	Main	Main
Step change	$\Delta x_F = -0.05$	$\Delta x_F = -0.05$	$\Delta F = -5.0\%$	$\Delta Q_B = -6.5\%$
Time elapsed (min)		20–60	10–40	10–40
v_Δ measured (tray/h)		7.8	9.9	−10.2
Wave Velocity Calculated with Measured Compositions and Flow Rates				
W' (mol/tray)	0.132	0.101	0.101	0.101
W'' (mol/tray)	0.128	0.128	0.132	0.132
v_Δ calculated (tray/h)	−106	9.5	12.1	−12.5
v_Δ error (tray/h)		1.7	2.2	−2.3
v_Δ error (%)		22	22	23
Wave Velocity Predicted by UMF Model				
$W'' = W'$ (mol/tray)	0.114	0.113	0.114	0.114
$L' = L''$ (mol/h)	40.0	40.0	37.9	40.0
$V'' = V'$ (mol/h)	25.1	25.1	25.2	23.5
V'' error (%)		3.0	1.6	−2.0
v_Δ predicted (tray/h)	−187	22.0	19.8	−21.7
v_Δ error (%)		182	100	113
Wave Velocity Predicted by CEW Model				
Q_L init. s.s. (kJ/h)		150	158	145
Without heat loss adjustment				
Q_L (kJ/h)	0	150	158	145
L' (mol/h)	40.8	42.5	40.5	41.2
V'' (mol/h)	24.9	24.9	25.3	23.4
V'' error (%)		2.1	2.0	−2.4
v_Δ predicted (tray/h)	−161	16.7	18.1	−19.7
v_Δ error (%)		114	83	94
With heat loss adjustment				
Q_L (kJ/h)	64	157	166	136
L' (mol/h)	42.2	42.7	40.6	41.0
V'' (mol/h)	23.3	24.7	25.1	23.6
V'' error (%)		1.4	1.2	−1.5
v_Δ predicted (tray/h)	−92	14.3	15.8	−17.2
v_Δ error (%)		84	60	69
Wave Velocity Predicted with Flow-Rate Disturbance				
L' (mol/h)			37.9	
V'' (mol/h)				23.5
v_Δ predicted (tray/h)			16.9	−18.3
v_Δ error (%)			71	80

model neglects the heat capacities of the trays and the column walls in the energy balance; these heat capacities tend to be relatively significant for small columns like ours.

For runs S3 and S5 with flow rate disturbances, the initial velocity of the resulting wave can also be predicted by using Eq. 1 with the column-end conditions at the initial steady state and the new flow rates. As Table 3 shows, such predictions for these two runs are roughly the same as those from the CEW model. This approach cannot be applied to run S1 because there was a delay, owing to the propagation of the composition disturbance, before the resulting wave was formed and began to travel.

Asymmetric Dynamics. Each pair of graphs in Figures 3–5 clearly demonstrates the asymmetric dynamics that the departure from a balanced steady state (S1, S3, S5) is always faster than the return to it (S2, S4, S6). In runs S2, S4 and S6, the exact final steady state (the balanced one) might not have been attained before we terminated the operation because the movement of the temperature profile was extremely slow near the end of each run. These results verified the qualitative nature of this interesting dynamic behavior as explained by the nonlinear wave theory (Hwang and Helfferich, 1989; Hwang, 1991). However, the dynamic asymmetry in these results appears to be not as severe as that from previous computer simulations. One reason is that we chose a relatively moderate system so that we could complete the slow return transition in a reasonable time period. In addition, nonidealities such as nonideal tray behavior and heat loss might have alleviated the dynamic asymmetry because they tend to loosen the pinches around the column ends.

Fractionation column dynamics

Table 2 lists the measured operating conditions at the initial and final steady states of our dynamic experiments F1–F6 on the 50-tray fractionation column. Because we focused on

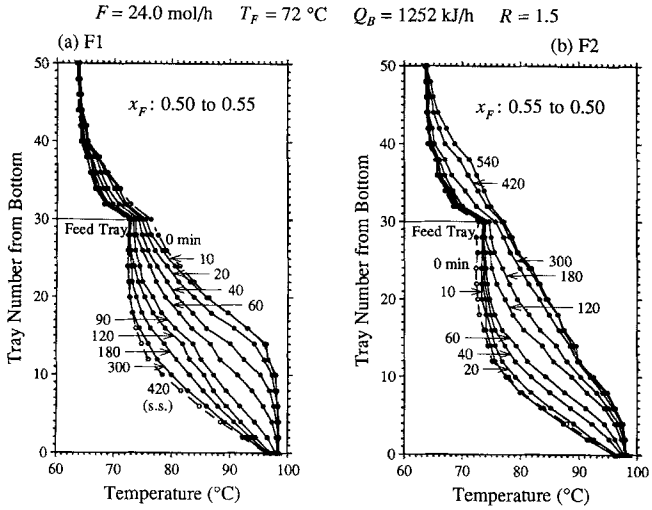

Figure 7. Temperature wave in fractionation column with methanol/1-propanol in response to step change of feed composition: (a) departure from balanced steady state; (b) return to balanced steady state.

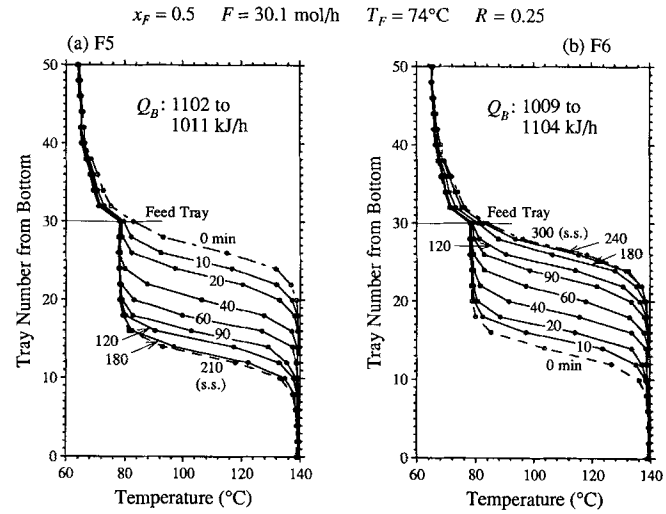

Figure 9. Temperature wave in fractionation column with methanol/1-pentanol in response to step change of reboiler heat supply: (a) departure from balanced steady state; (b) return to balanced steady state.

the behavior in the stripping section, all transitions were between steady states of types B and A. The recorded transient temperature profiles in these runs are shown by Figures 7–9, each consisting of a pair of graphs illustrating the departure and return to the balanced steady state B. Figure 7 reveals that, even with a relatively high reflux ratio (about 2.2 times of the minimum value), runs F1 and F2 with the methanol/1-propanol mixture reached only a marginally high-purity condition (the column-end pinches were not stable). Thus, we will focus our discussion on experiments F3–F6 with the methanol/1-pentanol mixture. For these runs, the histories of the measured distillate flow rates are given by Figure 10. For calculating the wave velocity in the stripping section, Table 2 also includes the measured column-end conditions during 10–40 min from the introduction of the step change in runs F3 and F5.

Constant-Pattern Wave. Figures 8 and 9 clearly demonstrate the propagation of a constant-pattern wave in the stripping section of our fractionation column. For all cases here, the travel of the wave in the rectifying section toward the feed location was insignificant. For the departure from the balanced steady state in runs F3 and F5, the initial stand-

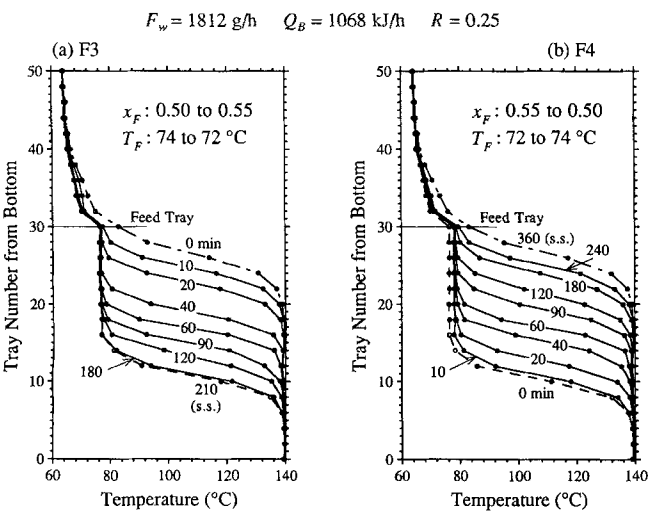

Figure 8. Temperature wave in fractionation column with methanol/1-pentanol in response to step change of feed composition with fixed-mass flow rate: (a) departure from balanced steady state; (b) return to balanced steady state.

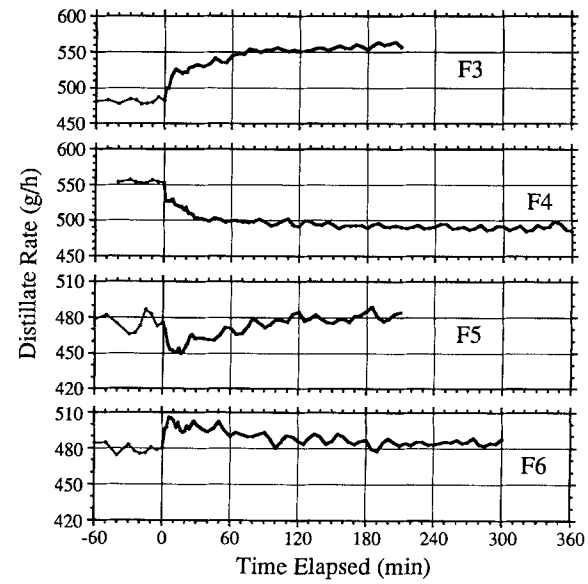

Figure 10. Histories of distillate rate in dynamic experiments on fractionation column with methanol/1-pentanol.

ing waves in both sections were around the feed tray. Thus, the disturbance of the feed composition in run F3 merged into the standing waves immediately and moved the profile downward. In run F5, the change of vapor flow rate introduced to the bottom end took negligible time to reach the initial standing wave, and the wave in the stripping section (the principal wave) began to travel downward almost immediately. According to the nonlinear wave theory, the principal wave in both cases would have traveled all the way to the bottom end and broken the pinch there if the column had been nearly adiabatic. However, there was a considerable heat loss from the stripping section because of the large temperature difference across the column wall (vacuum jacket). As the wave traveled downward, the temperatures in the stripping section decreased, and therefore the heat loss decreased. This increased the vapor flow rate and hindered the downward travel of the wave. An evidence for the decrease of the heat loss is the increase of the distillate rate (after the step change effect) during the travel of the wave, as shown by Figure 10. In both of these runs, the wave traveled at a constant velocity within the first 40 min of each transition.

In run F4, a disturbance of the feed composition was introduced to the initial steady state of type A. Figure 8b reveals the propagation of the disturbance wave on the background of the initial standing wave and their merger to form a new wave (see the temperature profiles at 0 and 10 min), as predicted by the nonlinear wave theory.

Wave Velocity. To control a fractionation column subject to disturbances at a balanced steady state, one is primarily interested in the initial velocity of the principal wave immediately after the balanced condition is perturbed. For runs F3 and F5, this initial wave velocity remained virtually constant in the first 40 min (see Figures 8a and 9a), in spite of the fact that the condition at the feed tray was varying during the first 10 min. The measured wave velocities based on the recorded temperature profiles are given in Table 4. According to the nonlinear wave theory, the velocity of this wave after the feed tray was pinched can be calculated with the compositions and flow rates at the ends of the stripping section. For this purpose, Table 2 also lists the section-end conditions measured over the period of 10–40 min of time elapsed as well as at the initial steady state. Using these measured data, we estimate the compositions and flow rates at the top end of the stripping section (immediately below the feed) with a vapor–liquid equilibrium model and material balances, and then calculate the wave velocity with Eq. 1 (see Appendix C for details). As Table 4 indicates, the calculated velocity is slightly higher (in absolute value) than the measured one for both runs F3 and F5, much as for the stripping column discussed earlier. With the same approach, we also calculate the standing wave velocity (supposed to be zero) at the initial steady state to check errors from measurement and physical-property models; this leads to virtually perfect standing waves in these runs, as shown by Table 4.

Table 4. Velocities of Constant-Pattern Waves in Stripping Section of Fractionation Column

Run No. Wave	F3 Standing	F3 Traveling	F5 Standing	F5 Traveling
Step change		$\Delta x_F = +0.05$ $\Delta F = +5.7\%$		$\Delta Q_B = -8.3\%$
Time elapsed (min)	0	0–40	0	0–40
v_Δ measured (tray/h)	0.0	−11.5	0.0	−10.0
Wave velocity calculated with measured section-end conditions				
P'' (mm Hg)	751	751	746	746
$\tilde{T}'$ (°C)	78.8	73.4	79.1	75.0
$\tilde{x}'$	0.496	0.641	0.485	0.588
$\tilde{y}'$	0.931	0.959	0.930	0.950
$\tilde{L}'$ (mol/h)	2.4	2.1	2.3	2.0
$\tilde{V}'$ (mol/h)	17.4	18.5	17.2	16.3
x''	0.500	0.556	0.499	0.505
y''	0.931	0.959	0.930	0.950
L'' (mol/h)	32.4	33.5	32.2	31.7
V'' (mol/h)	17.4	18.5	17.2	16.3
W'' (mol/tray)	0.108	0.114	0.107	0.108
W' (mol/tray)	0.073	0.073	0.073	0.073
v_Δ calculated (tray/h)	0.5	−13.3	−1.3	−10.8
v_Δ error (tray/h)	0.5	−1.8	−1.3	−0.8
v_Δ error (%)		16		8
Wave velocity predicted by composite-wave approximation				
z_F	0.500	0.550	0.500	0.500
F_w (g/h)	1,805	1,805	1,794	1,794
F (mol/h)	30.0	31.5	29.9	29.9
x''	1.000	1.000	1.000	1.000
y''	1.000	1.000	1.000	1.000
L'' (mol/h)	3.8	3.8	3.7	3.7
V'' (mol/h)	18.8	18.8	18.6	17.0
W'' (mol/tray)	0.202	0.202	0.202	0.202
W' (mol/tray)	0.073	0.073	0.073	0.073
v_Δ predicted (tray/h)	0.1	−11.3	−0.3	−8.0
v_Δ error (tray/h)	0.1	0.2	−0.3	2.0
v_Δ error (%)		−2		−20

Prediction of Wave Velocity. To predict the velocity of the principal wave using only the information of the initial steady state and the step disturbance, one needs to predict the pinch condition at the feed location if the preceding approach is to be employed. Such a pinch composition can be predicted with an operating-line approach proposed previously (Hwang, 1991) if the molar flow rates of both liquid and vapor are uniform in each section. This ideal condition is unfortunately invalid for our column because of a considerable heat loss from the stripping section. Instead, we employed the composite-wave approximation presented in the Theory section. By neglecting the insignificant movement of the wave in the rectifying section, we assume the principal wave in the stripping section traveled at the average velocity of the composite wave, namely, the entire column profile. This average velocity is related to the compositions and flow rates at the column ends and of the feed by Eq. 6 (see Appendix C). As an error check, we first apply Eq. 6 to the initial steady state of runs F3 and F5; this leads to nearly perfect standing waves in both runs, as shown by Table 4. Then, for run F3, we impose the step change of the feed composition (accompanied by a change of molar flow rate at a fixed mass flow rate) on the initial steady-state condition to predict the initial wave velocity. For run F5, we translate the step change of the reboiler heat supply into step changes of both V' and V'' by assuming that the disturbance immediately affect the vapor flow rate proportionally throughout the column. As Table 4 shows, the predicted wave velocity agrees well with the measured one in both cases. It appears that this approach tends to underpredict the wave velocity, likely because it neglects the movement of the wave in the rectifying section.

Asymmetric Dynamics. The pairs of graphs in Figures 8 and 9 clearly exhibit the asymmetric dynamics that the departure from a balanced steady state of our fractionation column (runs F3 and F5) is always faster than the return to it (runs F4 and F6). Similar to that in the stripping column discussed earlier, the dynamic asymmetry is not as severe as that from previous computer simulations (Hwang, 1991), likely because of nonidealities such as nonideal tray behavior and heat loss.

Conclusions

A nonlinear wave theory was established previously (Hwang and Helfferich, 1988, 1989; Hwang, 1991, 1995) to provide better physical insight and a concise mathematical model of the nonlinear dynamic behavior of high-purity distillation columns. To test this theory, we have conducted dynamic experiments on a laboratory glass column with 50-mm sieve trays in two configurations: a 40-tray stripping column and a 50-tray fractionation column with a 30-tray stripping section. For investigating the fundamentals of wave-propagation dynamics, we used nearly ideal binary mixtures of methanol, 1-propanol, and 1-pentanol in the present study. With the aid of thermocouples on every other tray and a microcomputer system for data acquisition, we tracked the movement of the sharp temperature profile in response to a deliberately introduced step change of feed composition, feed flow rate, or reboiler heat supply. Focusing on a balanced steady state, which optimizes column utilization with respect to separation, we examined how the sharp profile moved in the fashion of a nonlinear wave when the balanced condition was perturbed by a disturbance as well as when it was restored. Our results can be summarized as follows:

- This study has provided an experimental observation of the dynamic behavior of a distillation column from a holistic point of view.
- This study has confirmed the existence of a constant-pattern wave in a high-purity distillation column, which was previously postulated for profile-position control (Luyben, 1972; Boyd, 1975; Silberberger, 1977; Gilles and Retzbach, 1980) and investigated theoretically (Marquardt, 1985, 1988; Hwang and Helfferich, 1988; Hwang, 1991).
- This study has demonstrated that the nonlinear wave theory satisfactorily predicts the velocity of the wave in the transition departing from a balanced steady state with discussions of possible error sources and appropriate levels of mathematical complexity.
- This study has verified the asymmetric dynamics that the departure from a balanced steady state is always faster than the return to it, as previously shown by computer simulations and explained by the nonlinear wave theory (Hwang and Helfferich, 1989; Hwang, 1991).

These results have fortified the nonlinear wave theory for applications to control and design of high-purity distillation columns. Prospective applications may include profile-position control, dual-composition control, feedforward control, control system analysis and synthesis, startup operation, and design of dynamically favorable columns.

Acknowledgments

We gratefully acknowledge the financial support of the National Science Foundation under grant CTS-9020749 and of Union Carbide Corporation. We are also indebted to Mr. M. Y. Nehme, Mr. D. J. Greene, and Ms. L. A. Patterson of Union Carbide for their help in our experimental work.

Notation

B = molar flow rate of bottoms (mol/h); as a subscript, bottoms or reboiler
D = molar flow rate of distillate (mol/h); as a subscript, distillate
D_w = mass (weight) flow rate of distillate (g/h)
F = molar flow rate of feed (mol/h); as a subscript, feed
h = molar enthalpy of liquid (kJ/mol)
H = molar enthalpy of vapor (kJ/mol)
L = molar flow rate of liquid stream (mol/h)
R = reflux ratio
T_k = tray (vapor) temperature for $k > 0$ and reboiler (vapor) temperature for $k = 0$ (°C)
U = molar vapor holdup (mol/tray)
v_Δ = shock wave velocity, defined in upward direction (tray/h)
V = molar flow rate of vapor stream (mol/h)
W = molar liquid holdup (mol/tray)
x = mole fraction of light component (methanol) in liquid
x_k = mole fraction of light component in liquid on (and leaving) tray k
x_B = mole fraction of light component in bottoms
x_D = mole fraction of light component in distillate
x_F = mole fraction of light component in liquid feed
y = mole fraction of light component (methanol) in vapor
y_k = mole fraction of light component in vapor on (and leaving) tray k
z_F = overall mole fraction of light component in feed (with one or two phases)
Δ = prefix for difference between two sides of shock wave
$\sim$ = rectifying section of fractionation column

Literature Cited

Boyd, D. M., "Fractionation Column Control," *Chem. Eng. Prog.*, **71**(6), 55 (1975).

Daubert, T. E., and R. P. Danner, eds., *The DIPPR Project 801 Data Compilation: Tables of Physical and Thermodynamic Properties of Pure Compounds*, Design Institute of Physical Property Data, AIChE, New York, NY (1991).
De Lorenzo, F., G. Guardabassi, A. Locatelli, and S. Rinaldi, "On the Asymmetric Behavior of Distillation Systems," *Chem. Eng. Sci.*, **27**, 1211 (1972).
Fair, J. R., "How to Predict Sieve Tray Entrainment and Flooding," *Petro./Chem. Engr.*, **33**(10), 45 (1961).
Fuentes, C., and W. L. Luyben, "Control of High-Purity Distillation Columns," *Ind. Eng. Chem. Proc. Des. Dev.*, **22**, 361 (1983).
Gilles, E. D., and B. Retzbach, "Reduced Models and Control of Distillation Columns with Sharp Temperature Profiles," *Proc. 19th IEEE Conf. Decision and Control*, Vol. 2, p. 860 (1980).
Gmehling, J., U. Onken, and W. Arlt, eds., *Vapor-Liquid Equilibrium Data Collection*, Vol. I, Parts 2a, 2b, and 2c, DECHEMA, Frankfurt/Main, Germany (1977).
Han, M., and S. Park, "Control of High-Purity Distillation Column Using a Nonlinear Wave Theory," *AIChE J.*, **39**, 787 (1993).
Hill, W. D., and M. Van Winkle, "Vapor-Liquid Equilibria in Methanol Binary Systems: Methanol-Propanol, Methanol-Butanol, and Methanol-Pentanol," *Ind. Eng. Chem.*, **44**, 205 (1952).
Howard, G. M., "Unsteady-State Behavior of Multicomponent Distillation Columns: II. Experimental Results and Comparison with Simulation During Start-Up at Total Reflux," *AIChE J.*, **16**, 1030 (1970).
Huckaba, C. E., F. P. May, and F. R. Franke, "An Analysis of Transient Conditions in Continuous Distillation Operations," *Chem. Eng. Prog. Symp. Ser.*, **59**(46), 38 (1963).
Hwang, Y.-L., "Nonlinear Wave Theory for Dynamics of Binary Distillation Columns," *AIChE J.*, **37**, 705 (1991).
Hwang, Y.-L., "On the Nonlinear Wave Theory for Dynamics of Binary Distillation Columns," *AIChE J.*, **41**, 190 (1995).
Hwang, Y.-L., and F. G. Helfferich, "Dynamics of Continuous Countercurrent Mass-Transfer Processes: II. Single-Component Systems with Nonlinear Equilibria," *Chem. Eng. Sci.*, **43**, 1099 (1988).
Hwang, Y.-L., and F. G. Helfferich, "Nonlinear Waves and Asymmetric Dynamics of Countercurrent Separation Processes," *AIChE J.*, **35**, 690 (1989).
Hwang, Y.-L., G. K. Graham, and G. E. Keller II, "An Experimental Study of Nonlinear Dynamics of Binary Distillation Columns," AIChE Meeting, Los Angeles, CA (1991).
Kapoor, N., T. J. McAvoy, and T. E. Marlin, "Effect of Recycle Structure on Distillation Tower Time Constants," *AIChE J.*, **32**, 411 (1986).
Luyben, W. L., "Control of Distillation Columns with Sharp Temperature Profiles," *AIChE J.*, **17**, 713 (1971).
Luyben, W. L., "Profile Position Control of Distillation Columns with Sharp Temperature Profiles," *AIChE J.*, **18**, 238 (1972).
Marquardt, W., "Model Reduction Techniques for Separation Columns," *Proc. Int. Conf. Industrial Process Modeling and Control*, Hangzhou, China (1985).
Marquardt, W., "Nonlinear Model Reduction for Binary Distillation," *IFAC Proc. Dynamics and Control of Chemical Reactors and Distillation Columns*, p. 123 (1988).
Mizuno, H., Y. Watanabe, Y. Nishimura, and M. Matsubara, "Asymmetric Properties of Continuous Distillation Column Dynamics," *Chem. Eng. Sci.*, **27**, 129 (1972).
Moczek, J. S., R. E. Otto, and T. J. Williams, "Approximation Models for the Dynamic Response of Large Distillation Columns," *Chem. Eng. Prog. Symp. Ser.*, **61**(55), 136 (1965).
Rose, A., C. L. Johnson, and T. J. Williams, "Transients and Equilibration Time in Continuous Distillation," *Ind. Eng. Chem.*, **48**, 1173 (1956).
Silberberger, F., "Simulation and Control of an Extractive Distillation Column," *5th Proc. Symp. Comput. Chem. Eng.*, p. 415 (1977).
Skogestad, S., and M. Morari, "The Dominant Time Constant for Distillation Columns," *Comput. Chem. Eng.*, **11**, 607 (1987).
Stathaki, A., D. A. Mellichamp, and D. E. Seborg, "Dynamic Simulation of a Multicomponent Distillation Column with Asymmetric Dynamics," *Can. J. Chem. Eng.*, **63**, 510 (1985).
Weigand, W. A., A. K. Jhawar, and T. J. Williams, "Calculation Method for the Response Time to Step Inputs for Approximate Dynamic Models of Distillation Columns," *AIChE J.*, **18**, 1243 (1972).

Appendix A: Physical Properties

The physical properties of the three alcohols and their binary mixtures used in our experiments are listed in Table A1. We gathered the compound properties from the DIPPR databank (Daubert and Danner, 1991) and the parameters of the UNIQUAC model for liquid activity coefficients in mixtures from the DECHEMA databank (Gmehling et al., 1977). We assume all vapors to be ideal gases. Accordingly, the vapor enthalpy of a compound is an integral of the ideal-gas heat capacity from a reference temperature (25°C), at which the gaseous atomic state is chosen as the datum of enthalpy. We calculate the liquid enthalpy of a compound from its vapor enthalpy and heat of vaporization with the assumption of no pressure effect on enthalpies. We assume the enthalpy of a mixture in either phase to be the molar average of its component enthalpies in that phase.

To calculate the vapor–liquid equilibrium properties of a binary mixture, we employ the liquid activity coefficients $\{\gamma_i\}$ predicted using the UNIQUAC model (which is chosen for consistency with potential extensions to multicomponent systems in the future). This model gives $\{\gamma_i\}$ in the range of 1.0–1.04 for methanol/1-propanol and of 1.0–1.2 for methanol/1-pentanol in the composition range of interest ($x = 0$–0.5). As a result, a bubble-point calculation following Raoult's law (ideal mixture, $\gamma_1 = \gamma_2 = 1$) leads to lower y values by merely 0.001–0.006. A further simplification by assuming a constant relative volatility (using an average value) incurs another slight underestimation of y by 0.001–0.002. For the methanol/1-propanol mixture, however, even the calculation with $\{\gamma_i\}$ underpredicts y around $x = 0.5$ by 0.014 compared with our measured values, which agree well with a published result (Hill and Van Winkle, 1952). Because this error is significant relative to a disturbance of only 5–10% in our stripping-column experiments, we present the wave-velocity prediction using our measured vapor–liquid equilibrium data. For calculating the wave velocity in our fractionation-column experiments with methanol/1-pentanol, we rely on the vapor–liquid equilibrium calculation with $\{\gamma_i\}$, which provides a good prediction of the equilibrium properties (the simplified ways are also satisfactory).

Appendix B: Wave Velocity in Stripping Column

The stripping-column experiments S1, S3, and S5 exemplify a dynamic transition departing from a balanced steady state. We are primarily interested in the velocity of the resulting wave when it was just formed from the merger of the disturbance wave with the original standing wave. For run S1 with a feed composition disturbance, the velocity of the disturbance wave is also useful. We neglect the vapor holdup in all calculations because it is much smaller than the liquid holdup in our column.

Calculation with measured column-end conditions

For a wave in a stripping column, one can calculate its velocity using Eq. 1 with the column-end conditions, as discussed in the Theory section. Since the bottom end was pinched, $x' = y' = x_B$. The leaving liquid rate L' is of no consequence in our cases because x' is essentially zero. We calculate the entering vapor rate V' using the measured Q_B and

Table A1. Physical Properties of Methanol, 1-Propanol, 1-Pentanol, and Their Binary Mixtures

Compound	Methanol	1-Propanol	1-Pentanol
Molecular weight	32.042	60.096	88.150
Normal boiling point (°C)	64.7	97.2	137.8
Heat of vaporization (ΔH_i^* in kJ/mol, T in K): $\Delta H_i^*(T) = A(1-T/T_c)^B$			
T_c (critical temperature)	512.64	536.78	586.15
A	52.390	63.300	83.100
B	0.36820	0.35750	0.51100
Vapor enthalpy (H_i in kJ/mol, T in K, $T^\circ = 298$ K): $H_i(T) = H_i^\circ + A(T-T^\circ) + BC\left(\coth\frac{C}{T} - \coth\frac{C}{T^\circ}\right) - DE\left(\tanh\frac{E}{T} - \tanh\frac{E}{T^\circ}\right)$			
H_i° (heat of formation at T°)	−200.94	−255.20	−298.74
A	0.039252	0.061900	0.090600
B	0.087900	0.20213	0.30620
C	1,916.5	1,629.3	1,605.4
D	0.053654	0.12956	0.21150
E	896.70	727.40	−717.97
Liquid enthalpy (h_i in kJ/mol, T in K): $h_i(T) = H_i(T) - \Delta H_i^*(T)$			
Vapor pressure (p_i in Pa, T in K): $p_i(T) = \exp(A + B/T + C\ln T + DT^E)$			
A	81.768	88.134	168.96
B	−6,876.0	−8,498.6	−12,659
C	−8.7078	−9.0766	−21.366
D	7.1926×10^{-6}	8.3303×10^{-18}	1.1591×10^{-5}
E	2	6	2
Parameters for UNIQUAC model of liquid activity coefficients of mixtures:			
r_i	1.4311	2.7799	4.1287
q_i	1.4320	2.5120	3.5920
Binary Mixture		Methanol/1-Propanol	Methanol/1-Pentanol
Vapor enthalpy (kJ/mol): $H = y_1H_1 + y_2H_2$			
Liquid enthalpy (kJ/mol): $h = x_1h_1 + x_2h_2$			
Liquid activity coefficients (UNIQUAC model, T in K; $i, j = 1, 2$ or 2, 1): $\gamma_i = \exp\left\{\ln\frac{\phi_i}{x_i} + \frac{z}{2}q_i\ln\frac{\phi_i}{\theta_i} + \phi_j\left(l_i - \frac{r_i}{r_j}l_j\right) - q_i\ln(\theta_i + \theta_j\tau_{ji}) + \theta_j q_i\left(\frac{\tau_{ji}}{\theta_i + \theta_j\tau_{ji}} - \frac{\tau_{ij}}{\theta_j + \theta_i\tau_{ij}}\right)\right\}$ where $l_i = \frac{z}{2}(r_i - q_i) - (r_i - 1) \quad z = 10$ $\phi_i = \frac{x_i r_i}{x_1r_1 + x_2r_2} \quad \theta_i = \frac{x_i q_i}{x_1q_1 + x_2q_2}$ $\tau_{ij} = \exp\left(\frac{-A_{ij}}{RT}\right) \quad R = 8.314$ J/mol/K			
A_{12} (J/mol)		−347.027	−228.046
A_{21} (J/mol)		757.986	1,387.67

the heat of vaporization at the composition x_B and temperature T_0 in the reboiler. At the top end, $x'' = x_F$, $L'' = F$, $y'' = x_D$, and $V'' = D$. For the molar liquid tray holdups, we estimate W' and W'' by assuming uniform liquid mass (weight) holdups on all trays. We employed an average column holdup (243 g) from all six runs instead of the individual value for each run to obtain an average tray holdup (6.075 g/tray). We first apply Eq. 1 to the initial steady state to calculate the standing wave velocity (supposed to be zero) for checking experimental errors. For the main traveling wave in the transition, we follow the same procedure but use the column-end compositions and flow rates measured during the transition as listed in Table 1. For the disturbance wave entering the top end in run S1, the upper-side conditions are the new top-end conditions, while the lower-side ones are the original top-end conditions except that L' is estimated by assuming a steady-state overall material balance around the disturbance wave.

Prediction by UMF model

To predict the wave velocity with the UMF model, we assume that L'' as well as L' are the same as the feed rate F at the initial steady state for runs S1 and S5 and as the new F for run S3; we also assume that V'' as well as V' are the same as the distillate rate at the initial steady state for runs S1 and S3, and are 6.5% lower than the steady-state value for run S5 owing to the 6.5% decrease of Q_B. For consistency in material balance, we have to assume $W' = W''$ with the value calculated from an average mole fraction $(x' + x'')/2$ and an

average mass tray holdup obtained from the measured mass-column holdup.

Prediction by CEW model

For the application of the CEW model to our cases, $x' = y' = x_B$ as mentioned before, while y'' is obtained from a measured value in equilibrium with x'' at P''. With these compositions, we evaluate the vapor and liquid enthalpies at the column ends using the models given in Table A1 for the initial steady states of all three runs and the transition of run S1 with the new feed composition. For W' and W'', we follow the same way as in the calculation of wave velocity with measured column-end conditions. Then, we take the energy balance into account to predict the two exiting flow rates V'' and L' in two steps.

The first step is to estimate the heat loss Q_L. Since we are interested in the velocity of the resulting wave when it was just formed, the temperature profile at that moment is fairly close to that at the initial steady state. By neglecting the small change of the column heat loss due to the disturbance wave, we assume the heat loss Q_L is the same as that at the initial steady state, which can be calculated with the following material and energy balances (note V'' here was measured):

$$L' = L'' + V' - V'' \tag{A1}$$

$$Q_L = V'H' - L'h' - V''H'' + L''h'' \tag{A2}$$

In the second step, Q_L can be inserted in Eq. 3 unless there is a reason for an adjustment, such as the one discussed earlier. As a result, Eq. 5 can be expanded into a set of two linear equations (note that L'' and V' are the new flow rates in runs S3 and S5, respectively):

$$\left(\frac{1}{A} - \frac{x'}{C}\right)L' + \left(\frac{1}{A} - \frac{y''}{C}\right)V'' = \left(\frac{V' + L'}{A} - \frac{V'y' + L''x''}{C}\right) \tag{A3}$$

$$\left(\frac{1}{A} - \frac{h'}{E}\right)L' + \left(\frac{1}{A} - \frac{H''}{E}\right)V'' = \left(\frac{V' + L''}{A} - \frac{V'H' + L''h'' - Q_L}{E}\right), \tag{A4}$$

where

$$\begin{aligned} A &\equiv (W'' + U'') - (W' + U') \\ C &\equiv (W''x'' + U''y'') - (W'x' + U'y') \\ E &\equiv (W''h'' + U''H'') - (W'h' + U'H'). \end{aligned} \tag{A5}$$

Now, V'' and L' can be solved from Eqs. A3 and A4 and then substituted in either Eq. 1, 3 or 4 to calculate the wave velocity.

Prediction with flow-rate disturbance

For run S3 with a disturbance of the feed flow rate, the initial wave velocity can also be predicted by using Eq. 1 with the new L'' (and L' changed accordingly) along with all other values the same as at the initial steady state, as mentioned in the Theory section. This is also applicable to run S5 with a disturbance of the reboiler heat supply by using the new V' and V'', which are reduced by 6.5% from the steady-state values owing to the 6.5% decrease of Q_B.

Appendix C: Wave Velocity in Fractionation Column

For our fractionation column experiments F3 and F5, we are interested in the initial velocity of the wave in the stripping section. This initial velocity can typically be approximated by the velocity when a pinch at the feed location was just established, as supported by our experimental results shown by Figures 8a and 9a. To calculate such a wave velocity using the measured section-end conditions, we need to evaluate the unmeasured flow rates and compositions at the top end of the stripping section.

Calculation with measured section-end conditions

To estimate the compositions and flow rates at the pinched feed location, we first exploit the material balances around the rectifying section (to be denoted by an overhead ˜). After the feed location had been pinched, the profile in the rectifying section remained the same; in other words, the wave velocity in that section was zero. Accordingly, application of Eqs. 1 and 4 to this standing wave gives

$$\tilde{V}''\tilde{y}'' - \tilde{L}''\tilde{x}'' = \tilde{V}'\tilde{y}' - \tilde{L}'\tilde{x}' \tag{A6}$$

$$\tilde{V}'' - \tilde{L}'' = \tilde{V}' - \tilde{L}'. \tag{A7}$$

The top-end compositions and flow rates are directly related to the measured distillate composition and flow rate ($\tilde{x}'' = \tilde{y}'' = x_D$, $\tilde{L}'' = RD$, $\tilde{V}'' = \tilde{L}'' + D$). For the bottom end, $\tilde{x}'$ is the same as that on the bottom tray of the rectifying section (tray 31), and therefore is calculated from the pressure ($\tilde{P}' = P''$) and temperature ($\tilde{T}' = T_{31}$) there using the vapor–liquid equilibrium model given in Table A1. Having observed that the trays in the rectifying section were very lightly loaded, we estimate P'' by assuming the pressure drop across the rectifying section to be only one tenth (about 2 mm Hg) of that across the entire column (24 mm Hg). For the temperature, we assume $T_{31} = (T_{30} + T_{32})/2$. For the vapor entering the rectifying section, $\tilde{y}'$ can be computed from the information of the vapor leaving the stripping section and the feed. With a nearly saturated liquid feed as in our experiments, $\tilde{y}'$ is approximately the same as the composition y'' of the vapor leaving the feed tray (tray 30). We calculate y'' from P'' and T_{30} using the vapor–liquid equilibrium model. With $\tilde{x}'$ and $\tilde{y}'$, we can solve $\tilde{L}'$ and $\tilde{V}'$ from Eqs. A6 and A7.

With the assumption of a saturated liquid feed, the composition x'' and flow rates L'' and V'' at the top end of the stripping section can be obtained by using the material balances around the feed location:

$$V'' = \tilde{V}' \qquad L'' = F + \tilde{L}' \qquad x'' = \left(Fx_F + \tilde{V}'\tilde{x}'\right)/L''. \tag{A8}$$

For the bottom end, the boilup vapor rate V' is directly related to the reboiler heat supply Q_B. Since the bottom end was still pinched at the moment of interest, it follows that $x' = y' = x_B$. Since $x_B = 0$ for a high-purity column, the liquid flow rate L' is inconsequential for calculating the wave velocity. We neglect all vapor holdups and the liquid holdups in the very lightly loaded rectifying section, and assume that the measured liquid mass holdup of the whole column (194 g, the average from the four runs F3–F6) is uniformly distributed among all trays in the stripping section (6.467 g/tray). With these data, we calculate the wave velocity in the stripping section with Eq. 1. We also apply this approach to the initial balanced steady state to calculate the standing wave velocity (supposed to be zero) for checking measurement errors.

Prediction by composite-wave approximation

To apply the composite-wave approximation to runs F3 and F5, we calculate the average velocity of the composite wave with Eq. 6. For this, the bottom-end conditions are the same as in the preceding calculation while the top-end conditions can be related to the distillate conditions ($x'' = y'' = x_D$, $L'' = RD$, $V'' = L'' + D$). Since we used a liquid feed, $z_F = x_F$. Because the wave traveled mainly in the stripping section, we calculate the molar liquid holdup W'' on the upper side of the composite wave with x_D and the mass tray holdup in the stripping section (6.467 g/tray), instead of that in the rectifying section (nearly zero), as discussed in the Theory section.

Manuscript received Nov. 6, 1995, and revision received Mar. 1, 1996.